

7B.4 An Examination of the Structure of Three Tornadoes Using High-Frequency Ka-band Mobile Doppler Radar

Ryan S. Metzger*, Christopher C. Weiss, and Anthony E. Reinhart
Texas Tech University, Lubbock, TX

1. INTRODUCTION

In order to help mitigate loss of life as well as damage from a tornado it is necessary to understand both tornadogenesis as well as the wind field structure of tornadoes of different sizes. Knowledge of tornado structure is particularly important as it will enable engineers to design buildings that are better able to withstand tornadoes as well as protect the occupants within. The improved understanding of both tornadogenesis and tornado structure are central goals of two major tornado research field campaigns: the Verification of the Origins of Rotation in Tornadoes Experiment (VORTEX; Rasmussen et al. 1994), and its more recent successor, VORTEX2 (Bluestein et al. 2009; Wurman et al. 2010). Significant technological advances in instrumentation, particularly in the field of radar, have occurred since the original VORTEX campaign, partially motivating VORTEX2 in 2009-2010.

This study uses high-resolution Ka-band radar data collected during the VORTEX2 field campaign by the two Texas Tech University Ka-band radars (Weiss et al. 2009) to examine the horizontal structure of three tornadoes. The overall goal of this study is to see how well the observed tornadoes, which were rather weak, compare to current conceptual models of tornado structure. The three tornadoes that will be looked at in this study are the May 18, 2010 Stinnett, TX tornado, the tornado near Tribune, KS on May 25, 2010 and the June 13, 2010 tornado just north of Booker, TX.

2. BACKGROUND

Traditionally, the tangential velocities within a tornado are approximated using a Rankine combined vortex model (e.g., Rankine 1901; Depperman 1947). Past radar studies (e.g., Tanamachi et al. 2007) have generated profiles of tangential velocity in actual tornadoes to compare to the conceptual Rankine vortex model using the Ground Based Velocity Track Display (GBVTD) technique of Lee et al. (1999). The consensus of these studies was that the tangential wind profile

did not vary exactly as a Rankine vortex. Tanamachi et al. (2007) noted that the profile varied as a Burgers-Rott vortex (Burgers 1948; Rott 1958). This type of vortex is marked with a smoother transition from solid body rotation to potential flow, eliminating the cusp like feature in the profile at the radius of maximum wind. Further, Kosiba and Wurman (2010) found that the rate of decay of the wind velocity outside the radius of maximum wind was not as fast as expected in the traditional Rankine vortex model.

Laboratory studies (e.g., Church et al. 1979) and computer simulations (e.g., Lewellen et al. 1997) of tornado-like vortices have shown that a single dimensionless ratio determines the wind field structure of a tornado: the swirl ratio (S). There are a few different equations that have shown up in the scientific literature to describe the swirl ratio, one of which is defined as:

$$S = (Rv_R) / (2hu_R) \quad (1)$$

where R is the updraft radius, v_R is the tangential velocity at R , u_R is the radial velocity at R and h is the depth of the inflow layer (Rotunno 1979). Studies (e.g., Church et al. 1979; Rotunno 1979) have found that for $S < 1$ the vortex exhibits a single vortex structure, while for $S \geq 1$ a multi-vortex structure is observed.

More recently, two studies have used data from the Doppler on Wheels radar (DOW; Wurman et al. 1997) to estimate the swirl ratio of large, multi-vortex tornadoes (Lee and Wurman 2005; Kosiba and Wurman 2010). These studies found swirl ratios of greater than one, which follows the conceptual model. There has not yet been a study published in the scientific literature that uses measurements obtained from radar data to calculate the swirl ratio of a single-vortex tornado (in other words, a tornado with a predicted swirl ratio of less than 1 based on the conceptual model put forth by Church et al. 1979).

3. METHODOLOGY

This study utilizes data collected during the VORTEX2 field project by the TTUKa radars. The TTUKa radars are well designed to perform fine-scale studies of atmospheric phenomena. A detailed discussion of the technical specifications of the TTUKa radar system can be found in Weiss et al.

* Corresponding author address: Ryan S. Metzger,
Texas Tech University, Atmospheric
Science Group, Department of Geosciences,
Lubbock, TX, 79409; e-mail: Ryan.Metzger@ttu.edu

(2009). After collection the data are first quality controlled using the SOLOII software package (Oye et al. 1995). Areas of aliased velocity data were unfolded. Areas where the vortex was obscured were identified as such areas were not useable in this study.

This study utilizes the GBVTD technique of Lee et al. (1999) to analyze the horizontal structure the three tornadoes. Although the GBVTD technique was designed to be used on tropical cyclones (e.g., Lee et al. 2000) it has been successfully employed in past studies of tornado vortex structure (Bluestein et al. 2003, 2007; Lee and Wurman 2005; Tanamachi et al. 2007; Kosiba and Wurman 2010).

The data were objectively analyzed using a bilinear interpolation scheme (e.g., Mohr et al. 1986) to create a Cartesian grid with a spacing of $\Delta x = \Delta y = 25\text{m}$ and $\Delta z = 10\text{m}$. The bilinear interpolation scheme was chosen to better compare the results to previous GBVTD studies.

The GBVTD algorithm is highly dependent on the selection of a vortex center, using the assumption of symmetry around the center point. Because of the sensitive nature of the selection, it is necessary to employ a pseudo-objective strategy to accurately determine the vortex center. All past GBVTD studies have utilized the GBVTD simplex center seeking algorithm described in Lee and Marks (2000), the algorithm used in this study.

After center selection, the VTD algorithm is applied to the data. The VTD algorithm takes the objectively analyzed Cartesian grid and the selected center and calculates azimuthally-averaged tangential and radial velocity. In addition, asymmetries or higher wave number components in the tangential velocity are calculated.

4. JUNE 13, 2010

On June 13, 2010 the VORTEX2 armada successfully intercepted a tornado in the eastern Oklahoma panhandle about 10 km northeast of the town of Booker, TX (hereafter referred to as the Booker tornado). TTUKa2 was able to perform PPI and RHI scans of this tornado from a range of between 5 and 9 km. All PPI scans of this tornado were done at a 0.5° elevation angle. The Booker tornado was rain-wrapped as viewed from the vantage point of the TTUKa radar which at times attenuated the radar data; thus, not all of the PPI scans collected could be used in the analysis of this case. Nevertheless, a quality PPI scan taken at 20:53:37 UTC (Fig. 1) was utilized to study the structure of this storm using the GBVTD procedure.

The first component of flow around the vortex that was analyzed was the axisymmetric

(wavenumber 0) component. The analysis identifies the radius of maximum wind at 175 m. Maximum azimuthally averaged winds in this case are 34.4 m s^{-1} (Fig. 2), in agreement with the EF0 rating assigned by the National Weather Service. Between the center of the vortex and the radius of maximum wind, the tangential velocity increases in a quasi-linear fashion consistent with a vortex that is in solid body rotation. Away from the radius of maximum wind, the analyzed tangential velocity decreases at a rate similar to the function $r^{0.5}$ which is a slower rate of decay than the function of r^{-1} that is associated with the decay of tangential velocities in the theoretical Rankine vortex.

According to reports from members of the VORTEX2 team who had a close, unobstructed view, the tornado at times displayed a multi-vortex structure, though it is not possible to assign the reports to the specific time used in the GBVTD analysis. However, GBVTD analysis reveals the presence of higher wavenumber component in the tangential velocity flow field (Fig. 3). The presence of multiple vortices is further supported by the profile of radial velocity (cf. Fig. 2), where outward motion extends from the center of the vortex to about radius of about 37 meters with inward motion outside this radius. In a single cell vortex, inward radial motion is expected for the entire vortex. An RHI taken through the outbound side of the tornado reveals ancillary wind maxima perhaps supportive of a multi-vortex type structure as well (Fig. 4).

5. MAY 25, 2010

On May 25, 2010 the VORTEX2 armada intercepted a short-lived rope tornado in the vicinity of Tribune, Kansas (hereafter referred to as the Tribune tornado). This tornado was rated as an EF-0 on the enhanced Fujita scale, and was one of several short-lived tornadoes that formed in the vicinity that day. The Tribune tornado was scanned by TTUKa2 for its 12 second life cycle. A single PPI scan of the tornado was performed while the condensation funnel was on the ground at 23:20:34 UTC.

The PPI scan from 23:20:34 UTC (Fig. 5) provides an excellent opportunity to study the horizontal structure of a short-lived, small tornado. The GBVTD analysis at 23:20:34 shows a vortex with a maximum axisymmetric tangential velocity of 27 m s^{-1} at a radius of 87.5 m away from the center of the vortex (Fig. 6) which is slightly below the lowest wind speed prescribed by the operational EF scale for an EF-0 tornado.

The vortex at 23:20:34 shows a linear increase in tangential wind velocity from the center

of the vortex to the radius of maximum wind consistent with the solid body rotation within the Rankine vortex model. From the radius of maximum wind out to a radius of 150 m there is a non-linear decrease in tangential velocity that is similar to the form of a Rankine vortex (r^{-1}) but the drop of is not quite as fast ($r^{-0.1}$). At 150 m the tangential velocity drops off very rapidly in a linear fashion.

The GBVTD analysis of the PPI scan from 23:20:17 (just before the tornado formed) shows that the pre-tornadic structure of this vortex is very similar to the structure of the tornado at 23:20:34, with the exception that the vortex was slightly weaker. At this time no visible condensation funnel was evident. The vortex had a maximum tangential velocity of 24.8 m s^{-1} at a radius of 87.5 m from the center of the vortex (Fig. 7a). The GBVTD procedure was also applied to the PPI scan from 23:21:02, the PPI scan immediately after the dissipation of the condensation funnel. This scan shows that the tangential velocity did not decrease appreciably after the dissipation of the condensation funnel. It can be argued that in this case a weakly-tornadic rotation is still present after the condensation funnel lifts (Fig. 7).

6. MAY 18, 2010

On May 18, 2010 (local time) the VORTEX2 armada sampled a high precipitation supercell thunderstorm in the northern Texas Panhandle. This section will focus on a brief tornadic circulation that was observed by TTUKa2 near the town of Stinnett, Texas over a 3 minute time period from 00:39:06 UTC to 00:41:54 UTC (hereafter referred to as the Stinnett tornado). During this time period TTUKa2 performed PPI scans at the 0.0° , 0.2° , and 0.5° elevation angles. The Stinnett tornado was very brief in duration; however, it represents a unique opportunity to study the entire lifecycle of a weak tornado, and examine the possible cause of its quick demise. In the minutes preceding tornadogenesis, a surge of higher velocity air impinges on the location of the developing vortex (Fig. 8). This surge is similar to the rear-flank downdraft (RFD) surge that was noted in the same storm earlier this day (Skinner et al. 2010). While the surge is present at all elevations scanned, the Doppler velocities associated with the surge are generally higher in the 0.5° elevation scans. At 00:39:21 the surge collides with the already present, broader scale rotation and a small, but intense vortex becomes evident (Fig. 8d).

The scan from 00:39:21 UTC was the first on which the GBVTD procedure was applied. This PPI scan was at an elevation angle of 0.2° , thus it is

indicative of conditions near the surface ($\sim 35 \text{ m AGL}$). The GBVTD derived tangential velocity at this time (Fig. 9) shows a maximum tangential velocity of 41 m s^{-1} at a radius of 50 m. The overall structure of this incipient vortex is rather unusual and does not conform at all to the Rankine vortex type structure typically seen in tornadoes. From the center of the vortex to the radius of maximum wind, the traditional linear increase in tangential velocity is present; however, outside the radius of maximum wind, there is a sharp linear decrease in velocity. Because of this atypical profile the derived profile of angular momentum is rather unusual: angular momentum decreases outside the radius of maximum wind (Fig. 10). The profile of radial velocity indicates net inward motion throughout the profile (Fig. 11), thus lower angular momentum air is advected inward. GBVTD analysis of PPI scans from 00:39:37, 00:39:51, and 00:40:25 (not shown) all show similar structure.

By 00:41:54 (Fig. 12) the circulation had become wider with lower velocity winds. A GBVTD analysis from this time (Fig. 13) shows that the radius of maximum wind was 125 m and the maximum tangential velocity was 14.6 m s^{-1} . The overall structure of tangential velocity has become closer to that of the ideal Rankine vortex, but the velocities observed were too weak to be considered tornadic. Considering the distribution of radial velocity and angular momentum prior to dissipation, it is theorized that the quick death of this tornado is a result of the inward transport of lower angular momentum air in to the center of the vortex.

The Stinnett tornado offers a chance to estimate the swirl ratio of a single vortex tornado using (1) due to the fact that inflow depth could be estimated from scans conducted at more than one elevation angle. Unfortunately, at the time of the analysis, inflow was present throughout the depth of the vortex resolved by the radar (approximately 70 m AGL), thus the depth of the inflow layer is unknown and the swirl ratio cannot be directly solved for. It is possible, however, to work backward to show that this predicted value is true given the fact that the inflow layer is persistent up to 70 m AGL. If (1) is turned into an inequality it is possible to calculate a value that h must be larger than in order for the swirl ratio to be less than one. Of the three remaining terms in (1), the updraft radius is the only term not directly calculated by GBVTD. In a laboratory simulated vortex, such as those used by Church et al. (1979) in the development of the swirl ratio, the updraft width is determined by the size of the updraft hole in the simulator, and thus is a constant. In a real tornado

the updraft width is variable over time and thus not easily defined. Using the profile of divergence (Fig. 14), 100 m was selected as the radius of the updraft as there is a significant drop off in convergence. At this radius tangential velocity is 13.5 m s^{-1} and the radial velocity is 8 m s^{-1} . Given an updraft radius of 100m, tangential velocity of 13.5 m s^{-1} , and a radial velocity of 8 m s^{-1} , the depth of the inflow layer must be larger than 84.4 m AGL in order to for the swirl ratio to be less than one. Given that the inflow layer is present at a height of 70 m this conclusion is very plausible. Past studies further support this assertion. For example, Church et al. (1979) noted that the value of h , the depth of the inflow layer, is typically 1 km and has a plausible range of between 0.5 and 2 km. In a GBVTD analysis of the May 3, 1999 Mulhall, Oklahoma tornado Lee and Wurman (2005) found the depth of the inflow layer to be highly variable over the life cycle of the tornado; however, the value was always between 0.5 and 1.0 km AGL.

7. CONCLUSIONS

Previous studies (e.g., Tanamachi et al. 2007; Kosiba and Wurman 2010) have shown that the Rankine vortex model does a good job at modeling the flow within the radius of maximum wind. These previous studies of large tornadoes have also shown that the transition from solid body rotation to potential flow is not a sharp transition, but rather a smooth one (similar to a Burgers-Rott vortex). This study shows that the findings in the previous studies can be extended to small tornadoes. It should be noted that a Burgers-Rott type vortex might take a while to develop after tornadogenesis as evidenced by the rather deviant profile exhibited by the incipient Stinnett tornado.

Past studies (e.g., Lee and Wurman 2005; Kosiba and Wurman 2010) that have attempted to calculate the swirl ratio of an actual tornado have only considered large, multi-vortex tornadoes. Before this study no one had ever used radar to estimate the swirl ratio of a small, single vortex tornado to see if indeed the value is less than one as expected. This study estimated the swirl ratio of the Stinnett tornado and found it highly probable that the swirl ratio is indeed less than one which agrees with the conceptual model put forth by Church et al. (1979). It should be noted that different interpretations of the updraft width could cause error in the estimation of swirl ratio presented in this study; however, all interpretations similarly yield a swirl ratio that is less than one.

8. ACKNOWLEDGEMENTS

The National Science Foundation provided funding for the radars to participate in the 2010 portion of the VORTEX2 field campaign through NSF grant AGS-0964088. Robin Tanamachi provided the GBVTD code as well as information on how to conduct the GBVTD analysis. Patrick Skinner, Brad Charboneau and Scott Gunter also provided valuable discussion about this study. The authors are grateful for the assistance of all of the faculty and students from Texas Tech University and the University of Michigan who assisted in the data collection during the VORTEX2 project.

9. REFERENCES

- Bluestein, H. B., W.-C. Lee, M. Bell, C. C. Weiss, and A. L. Pazmany, 2003: Mobile Doppler radar observations of a tornado in a supercell near Bassett, Nebraska, on 5 June 1999. Part II: Tornado-vortex structure. *Monthly Weather Review*, **131**, 2968-2984.
- Bluestein, H. B., C. C. Weiss, M. M. French, E. M. Holthaus, R. L. Tanamachi, S. Frasier, and A. L. Pazmany, 2007: The structure of tornadoes near Attica, Kansas, on 12 May 2004: High-Resolution, mobile, Doppler radar observations. *Monthly Weather Review*, **135**, 475-506.
- Bluestein, H. B., and Coauthors, 2009: VORTEX2: The Second Verification of the Origins of Rotation in Tornadoes Experiment. *5th European Conference on Severe Storms*, paper 09-06.
- Burgers, J. M., 1948: A mathematical model illustrating the theory of turbulence. *Adv. Appl. Mech.*, **1**, 197-199.
- Church, C. R., J. T. Snow, G. L. Baker, and E. M. Agee, 1979: Characteristics of tornado-like vortices as a function of swirl ratio: A laboratory investigation. *Journal of the Atmospheric Sciences*, **36**, 1755-1776.
- Depperman, C. E., 1947: Notes on the origin and structure of Philippine typhoons. *Bulletin of the American Meteorological Society*, **28**, 399-404.
- Kosiba, K., and J. Wurman, 2010: The three-dimensional axisymmetric wind field structure of the Spencer, South Dakota, 1998 tornado. *Journal of the Atmospheric Sciences*, **67**, 3074-3083.

- Lee, W.-C., and F. D. Marks, 2000: Tropical cyclone kinematic structure retrieved from single-Doppler radar observations. Part II: The GBVTD-simplex center finding algorithm. *Monthly Weather Review*, **128**, 1925-1936.
- Lee, W.-C., and J. Wurman, 2005: Diagnosed three-dimensional axisymmetric structure of the tornado on 3 May 1999. *Journal of the Atmospheric Sciences*, **62**, 2373-2393.
- Lee, W.-C., B. J.-D. Jou, P.-L. Chang, and S.-M. Deng, 1999: Tropical cyclone kinematic structure retrieved from single-Doppler radar observations. Part I: Interpretation of Doppler velocity patterns and the GBVTD technique. *Monthly Weather Review*, **127**, 2419-2439.
- Lee, W.-C., B. J. D. Jou, P.-L. Chang, and F. D. Marks, 2000: Tropical cyclone kinematic structure retrieved from single-Doppler radar observations. Part III: Evolution and structures of Typhoon Alex (1987). *Monthly Weather Review*, **128**, 3982-4001.
- Lewellen, W. S., D. C. Lewellen, and R. I. Sykes, 1997: Large-eddy simulation of a tornado's interaction with the surface. *Journal of the Atmospheric Sciences*, **54**, 581-605.
- Mohr, C. G., L. Jay Miller, R. L. Vaughan, and H. W. Frank, 1986: The merger of mesoscale datasets into a common cartesian format for efficient and systematic analyses. *Journal of Atmospheric and Oceanic Technology*, **3**, 143-161.
- Nelder, J. A., and R. Mead, 1965: A simplex method for function minimization. *Comput. J.*, **7**, 308-313.
- Oye, R., C. K. Mueller, and S. Smith, 1995: Software for radar translation, visualization, editing, and interpolation. *27th Conf. on Radar Meteorology*, Amer. Meteor. Soc., 359-361.
- Rankine, W. J. M., 1901: *A Manual of Applied Mechanics*. 16 ed. Charles Griff and Co., 680 pp.
- Rasmussen, E. N., J. M. Straka, R. Davies-Jones, C. A. Doswell, F. H. Carr, M. D. Eilts, and D. R. MacGorman, 1994: Verification of the Origins of Rotation in Tornadoes Experiment: VORTEX. *Bulletin of the American Meteorological Society*, **75**, 995-1006.
- Rott, N., 1958: On the viscous core of a line vortex. *Z. Angew. Math. Phys.*, **9**, 543-553.
- Rotunno, R., 1979: A study in tornado-like vortex dynamics. *Journal of the Atmospheric Sciences*, **36**, 140-155.
- Skinner, P. S., C. C. Weiss, A. E. Reinhart, W. S. Gunter, J. L. Schroeder, and J. Guynes, 2010: TTUKa mobile Doppler radar observations of near-surface circulations in VORTEX2. *25th Conference on Severe and Local Storms*, Amer. Meteor. Soc., paper 15.13.
- Tanamachi, R. L., H. B. Bluestein, W.-C. Lee, M. Bell, and A. Pazmany, 2007: Ground-Based Velocity Track Display (GBVTD) analysis of W-Band Doppler radar data in a tornado near Stockton, Kansas, on 15 May 1999. *Monthly Weather Review*, **135**, 783-800.
- Weiss, C. C., J. L. Schroeder, J. Guynes, P. S. Skinner, and J. Beck, 2009: The TTUKa mobile radar: Coordinated radar and in situ measurements of supercell thunderstorms during project VORTEX2. *34th Conference on Radar Meteorology*, Amer. Meteor. Soc.
- Wurman, J., L. Wicker, Y. Richardson, P. Markowski, D. Dowell, D. Burgess, and H. Bluestein, 2010: VORTEX2: The Verification of the Origins of Rotation in Tornadoes Experiment. *25th Conference on Severe and Local Storms*, Amer. Meteor. Soc., paper 5.1.

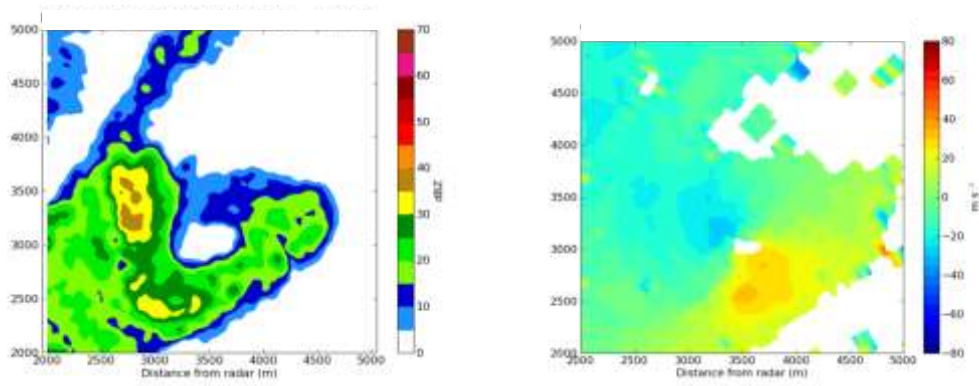


Figure 1. Objectively analyzed radar (right) reflectivity (dBZ) and (left) radial velocity (m s⁻¹) at 20:53:37 UTC.

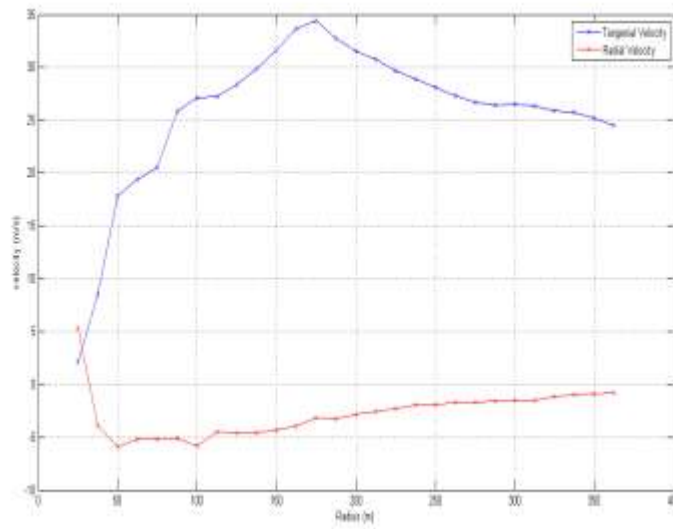


Figure 2. GBVTD-analyzed tangential (blue line) and radial (red line) velocity of the June 13, 2010 Booker tornado, valid at 20:53:37 UTC.

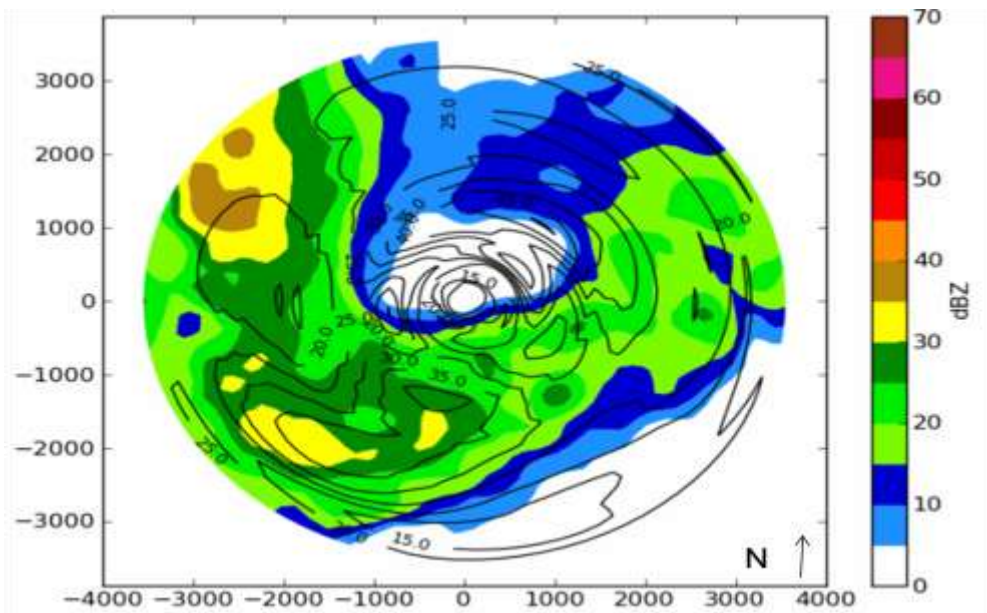


Figure 3. Reflectivity (dBZ, colored) with GBVTD derived tangential velocity (m s^{-1} , black contour lines with 5 m s^{-1} interval) showing higher wavenumber structure in the Booker tornado.

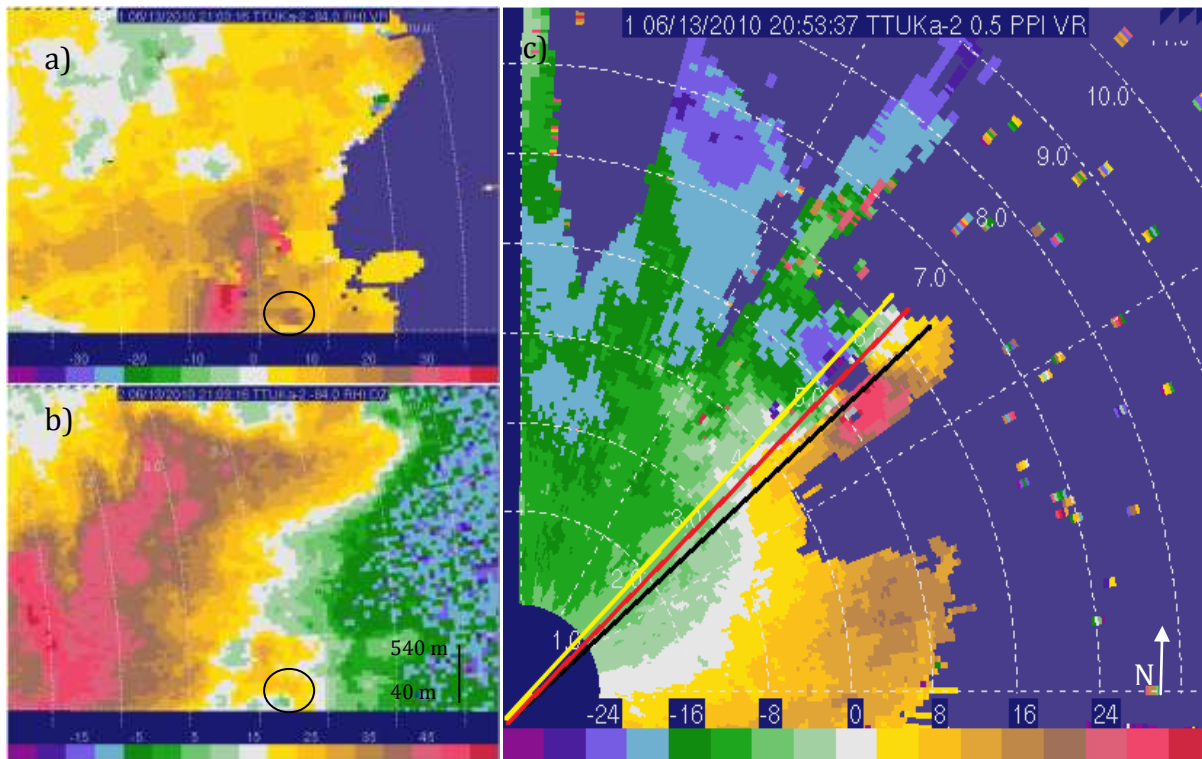


Figure 4. RHI image of a) Doppler velocity (m s^{-1}) and b) reflectivity (dBZ) showing possible evidence of a multiple vortex (circled) and c) a PPI showing the approximate plane of the RHI in a) and b) (black line).

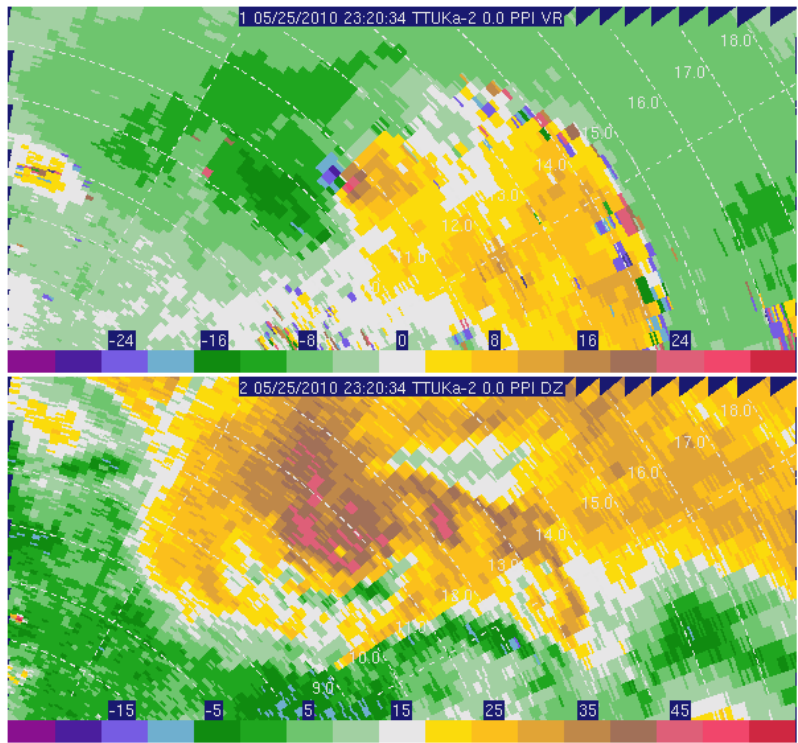


Figure 5. 0.0° PPI scan from 23:20:34 UTC of radial velocity (top; m s⁻¹) and reflectivity (bottom; dBZ).

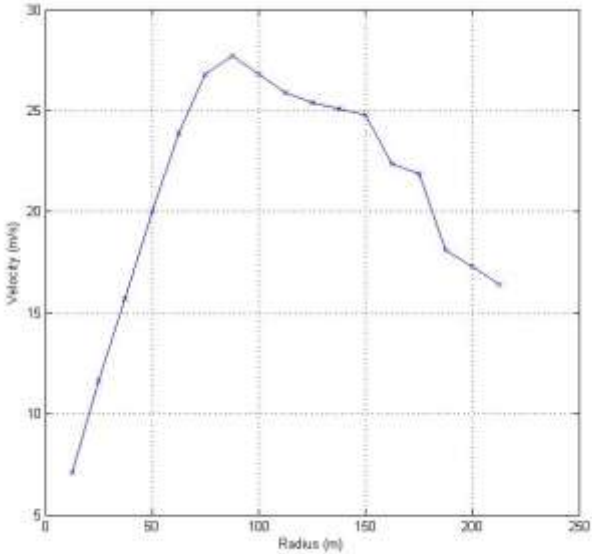


Figure 6. A GBVTD-derived profile of tangential velocity (m s⁻¹) at 23:20:34 UTC.

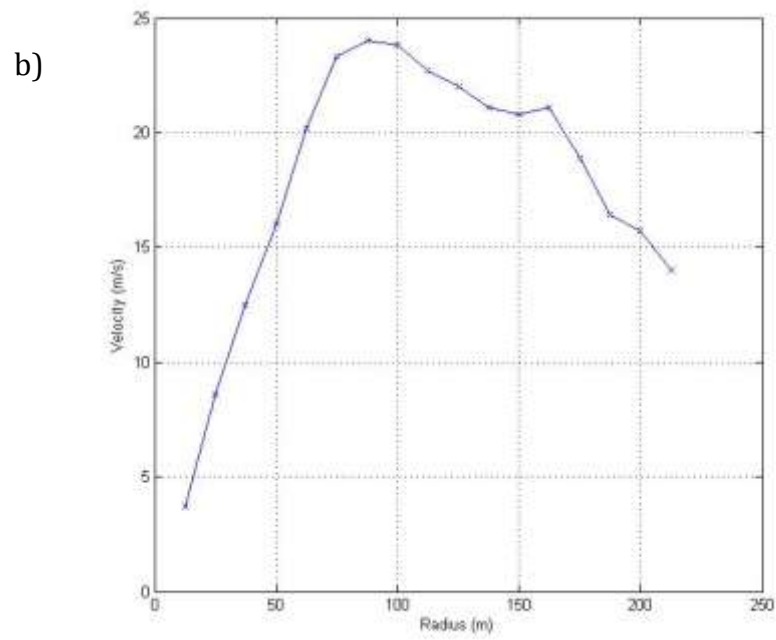
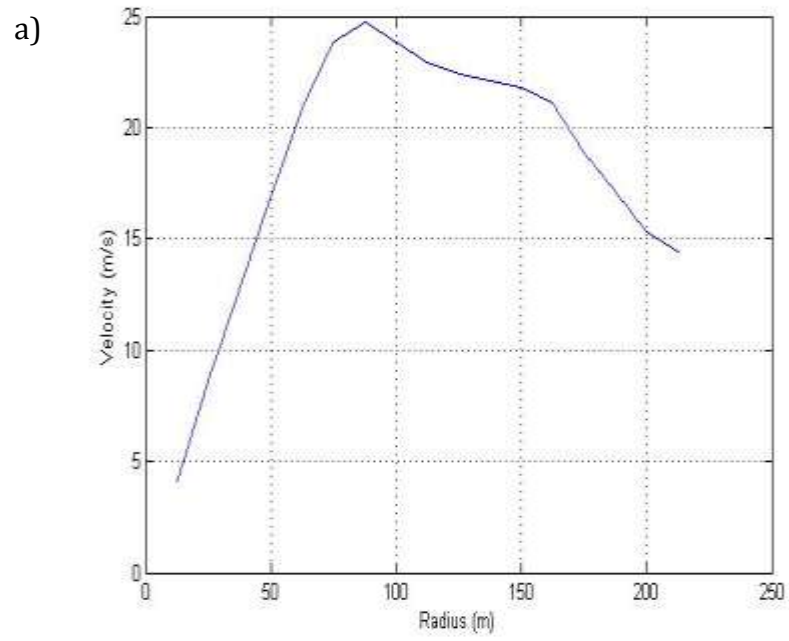


Figure 7. Same as Figure 4 but for a) 23:20:17 UTC and b) 23:21:02 UTC

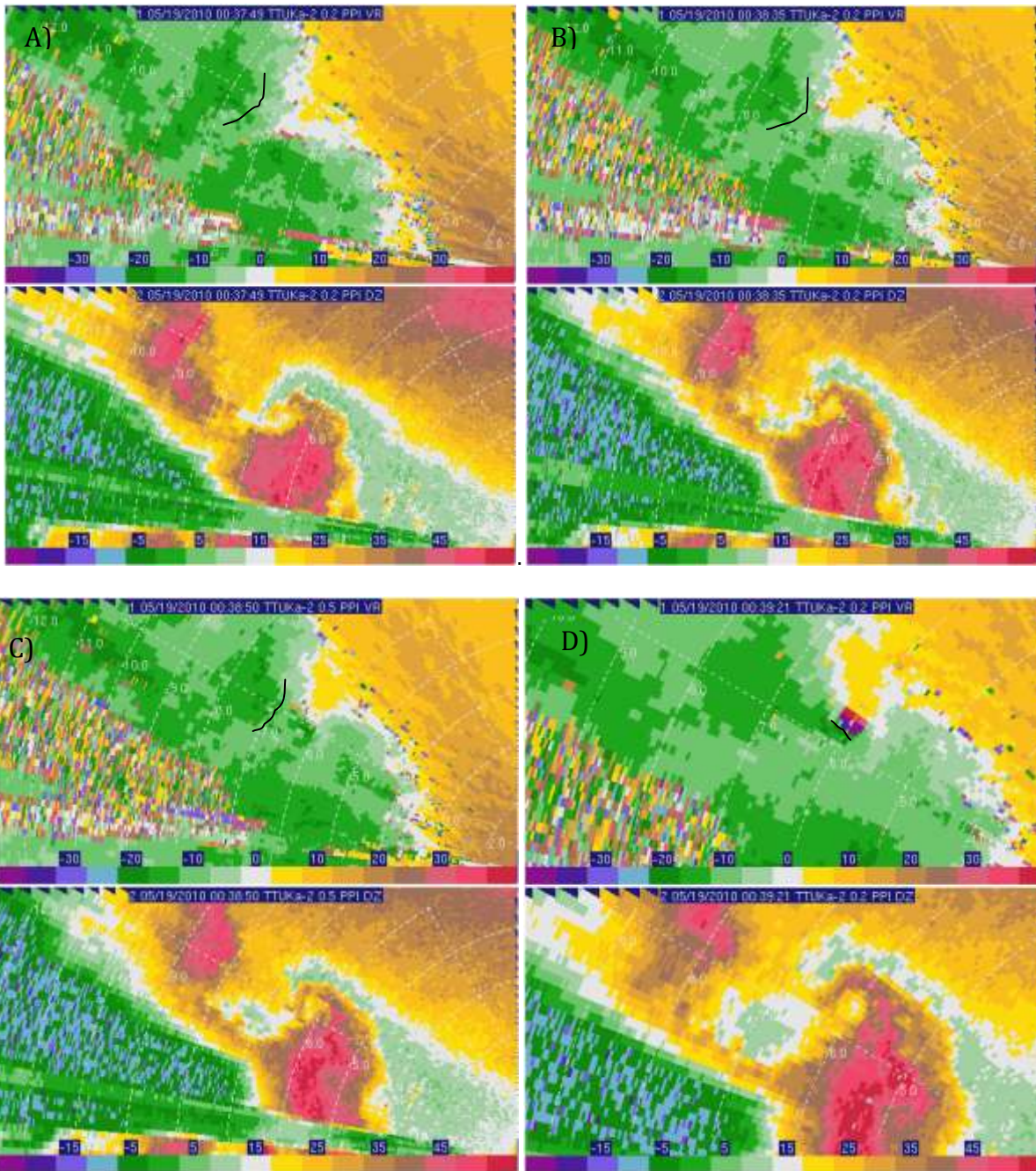


Figure 8. PPI scans from A) 00:37:49 UTC, B) 00:38:35 UTC, C) 00:38:50 UTC and D) 00:39:21 UTC of radial velocity (top; m s^{-1}) and reflectivity (bottom; dBZ). Black line shows the position of the rear flank gust front. Top of the figure is north, range rings are in 1000 m increments.

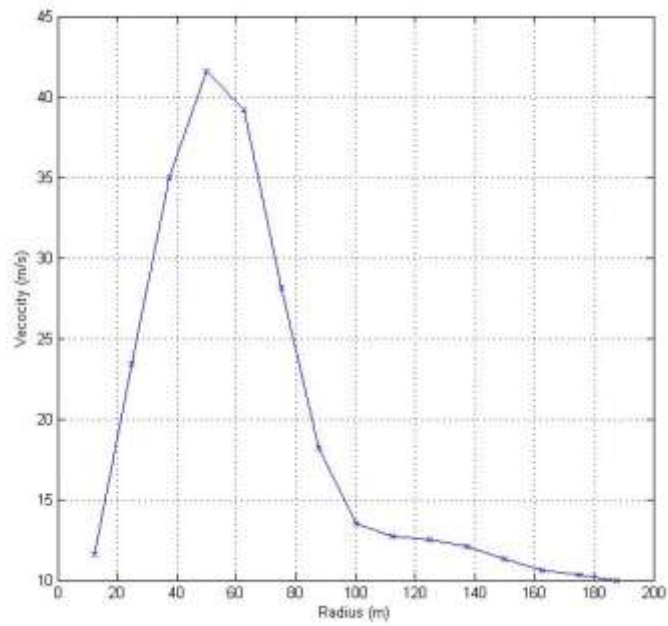


Figure 9. Profile of GBVTD-derived tangential (m s^{-1}) velocity at 00:39:21 UTC.

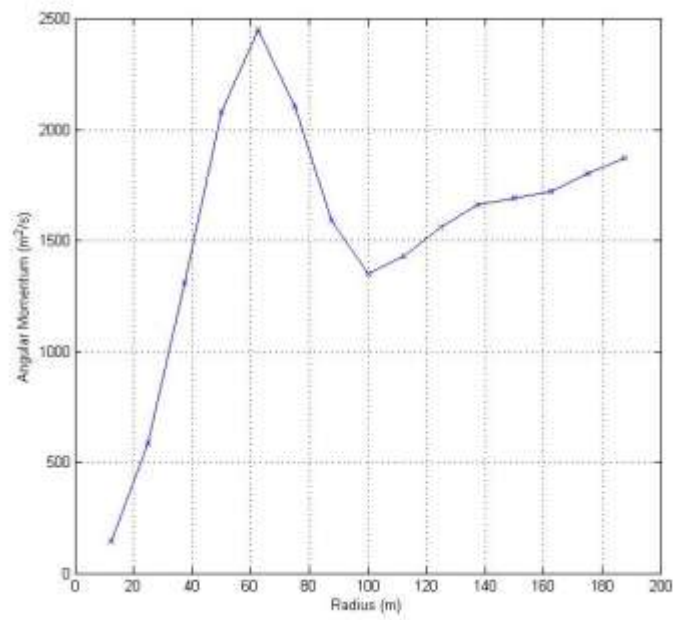


Figure 10. Profile of angular momentum ($\text{m}^2 \text{s}^{-1}$) at 00:39:21 UTC.

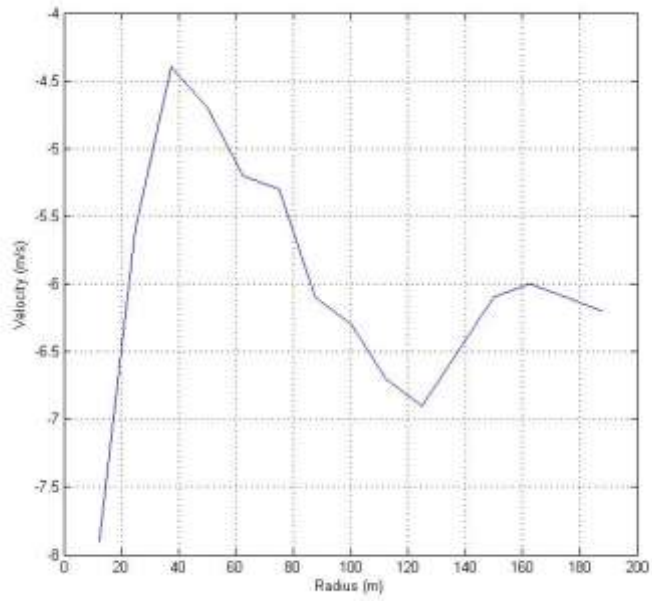


Figure 11. Profile of GBVTD derived radial velocity (m s^{-1}) at 00:39:21 UTC.

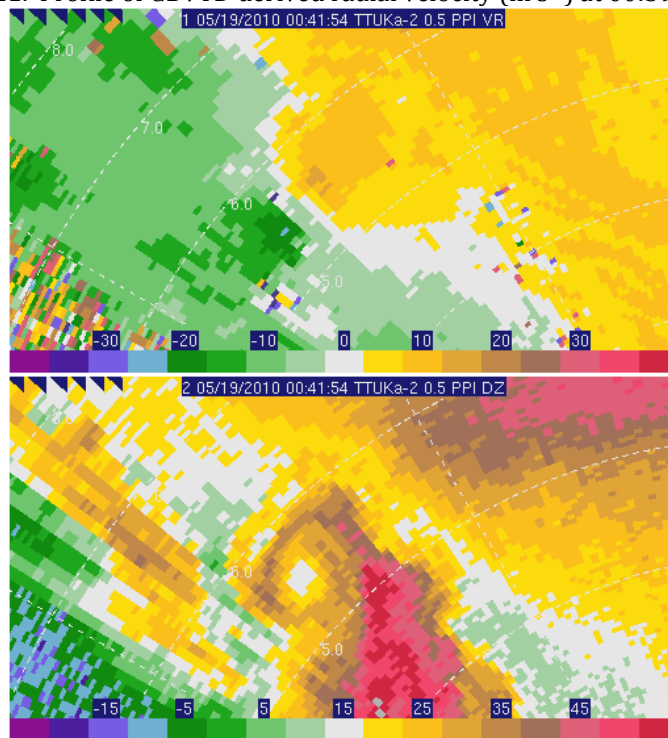


Figure 12. 0.5° PPI scan from 00:41:54 UTC of radial velocity (top; m s^{-1}) and reflectivity (bottom; dBZ). Top is north, range rings are in 1000 m increments.

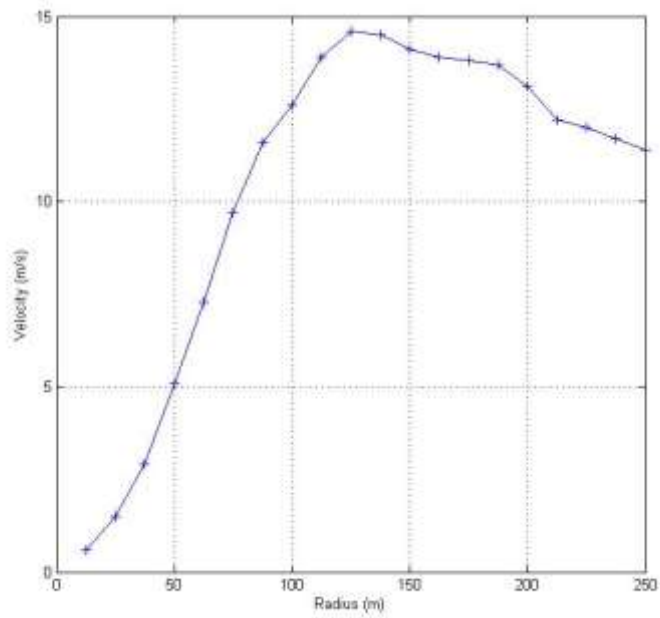


Figure 13. GBVTD-derived profile of tangential velocity (m s^{-1}) at 00:41:54 UTC.

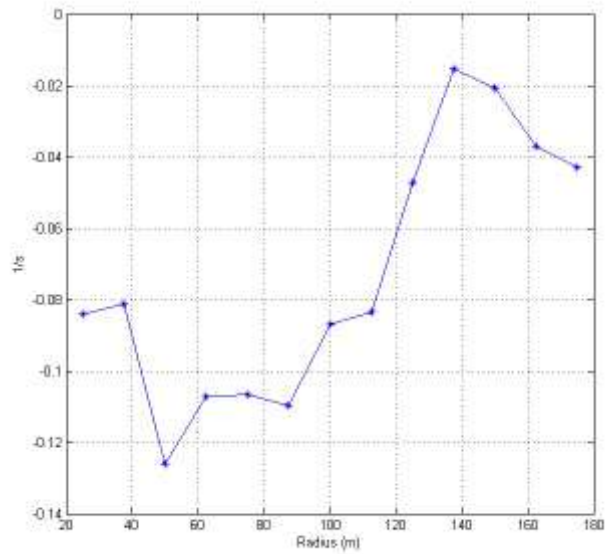


Figure 14. GBVTD-derived divergence (s^{-1}) for the Stinnett tornado at 00:39:21 UTC.

